Magnetic-field-induced substructures in multiple quantum wells consisting of magnetic and nonmagnetic semiconductor layers

S. Lee,* M. Dobrowolska, and J. K. Furdyna
Department of Physics, University of Notre Dame, Notre Dame, Indiana 46556

L. R. Ram-Mohan
Departments of Physics and Electrical and Computer Engineering, Worcester Polytechnic Institute, Worcester, Massachusetts 01609
(Received 21 July 1999)

We have investigated multiple quantum well systems consisting of diluted magnetic ($Zn_{1-x-y}Cd_xMn_ySe$) and nonmagnetic ($Zn_{1-x}Cd_xSe$) semiconductor wells, separated by nonmagnetic ZnSe barriers. By focusing on interband transitions involving the lowest multiplet of states (i.e., the ground state split by interwell interactions), we were able to study the details of the coupling between the wells. The strongest interaction between the states of each well occurs when the wells are identical (i.e., when they are in a resonant condition). The coupling between the wells is dramatically reduced in the presence of an external magnetic field, which can change the depth of diluted magnetic semiconductor (DMS) wells relative to the non-DMS wells via the large Zeeman splitting that occurs in the DMS layers. As soon as the depth of the wells becomes unequal, the multiple quantum well system subdivides into separate subsystems consisting of groups of equal (resonant) wells, one associated with non-DMS wells, and the other with DMS wells. This is clearly evident both from theoretical investigation and from the observed magnetic-field dependence of the absorption lines associated with the ground-state multiplet.

I. INTRODUCTION

One of the most interesting characteristics of II-VI-based diluted magnetic semiconductors (DMS's) is the giant Zeeman splitting[1,2] of electronic levels, which provides a relatively large tunability of the band edges by using an external magnetic field. This tunability has given rise to a large body of research on heterostructures, such as quantum wells (QW's) and superlattices (SL's), consisting in part of DMS layers.[3–10] For example, in some structures of this kind the zero-field valence-band offset can actually be overcome by the Zeeman shift of the valence-band edge in the DMS layers, and the band alignment of the system can thus be changed from type I to type II (or vice versa) simply by applying a magnetic field.[11,12] Using this mechanism, one can also produce so-called spin superlattices, in which different spin states are localized in different layers of the structure in the presence of an external magnetic field.[13–15]

Most studies using the giant Zeeman splitting in DMS layers have been done either on single QW or on SL structures, and significantly less attention has been given to coupled multiple QW's (specifically to QW systems consisting of more than two wells, such as triple or quintuple QW's).[16–18] At the same time there are many interesting and important features characteristic of coupled multiple quantum wells (MQW's), which can be very effectively investigated using DMS's. For example, a striking feature of coupled QW's is the wave-function distribution of their electronic states, since in symmetric MQW's wave functions of the lowest multiplet of states can be distributed within the system in a rather surprising manner, some of the states being localized only in certain wells and almost *entirely absent* in others. Such distribution of wave functions has already been mapped out in magnetoabsorption measurements carried out on MQW structures in which some layers consist of DMS's.[19] This interesting wave-function distribution, however, occurs only in the case of strong coupling between the wells (i.e., under resonant condition). To maintain this condition, in Ref. 19 the depth variation of DMS wells in an applied field was restricted to a small range (less than 10 meV), so that the system remained in nearly resonant condition through the entire experiment.

It is, however, also interesting to observe how the wave functions redistribute themselves when the system changes to off-resonant conditions (i.e., in the case of weak coupling between the wells) and how the coupling varies in the presence of large well depth variation. Even though some studies of interwell coupling in coupled systems have been reported, most of them have been done on double QW structures without involving DMS's (i.e., without the advantage of continuous tuning);[20–25] and, more importantly, these studies focused primarily on the dependence of coupling strength on the properties of the separating barriers (i.e., on their width and height).[26,27] It is obvious that the strength of the coupling between the wells is determined not only by the barrier properties, but also by the relative alignment of the wells themselves (i.e., whether or not the system is in a resonant condition). Such dependence of coupling on the relative well depth can be conveniently investigated in MQW's involving DMS wells, in which the band gap can be continuously varied relative to non-DMS wells.[28,29]

To explore this issue, in the present study we used symmetric MQW structures consisting of DMS ($Zn_{1-x-y}Cd_xMn_ySe$) and non-DMS ($Zn_{1-x}Cd_xSe$) wells, separated by nonmagnetic ZnSe barriers. Our aim is to explore the limit of strong Zeeman splitting, occurring at high magnetic field, when changes in the DMS well potentials produced by the applied field are on the same scale as the

TABLE I. Sample description.

Sample	Barrier	Non-DMS well	DMS well	L_w	L_b	x	y
TQW1	ZnSe	$Zn_{1-x}Cd_xSe$	$Zn_{1-x-y}Cd_xMn_ySe$	52 Å	20 Å	0.20	0.04
TQW2	ZnSe	$Zn_{1-x}Cd_xSe$	$Zn_{1-x-y}Cd_xMn_ySe$	38 Å	18 Å	0.20	0.04
QQW1	ZnSe	$Zn_{1-x}Cd_xSe$	$Zn_{1-x-y}Cd_xMn_ySe$	40 Å	20 Å	0.20	0.04
QQW2	ZnSe	$Zn_{1-x}Cd_xSe$	$Zn_{1-x-y}Cd_xMn_ySe$	40 Å	20 Å	0.21	0.04

well depth itself, leading to a transformation of the MQW systems into symmetric combinations of *unequal* wells. In this case, the system naturally divides into two subsystems having different well depths, one consisting of DMS wells and the other of non-DMS wells. While maintaining the condition of resonance within each subsystem, the two subsystems are now in off-resonant condition with respect to one another, the coupling between the two subsystems being significantly reduced. Thus each subsystem exhibits its own characteristic, nearly-independent behavior. By varying the magnetic field, we are able to continuously change the coupling process within the system as a whole, allowing us to investigate the transition from strong coupling between all wells to the situation when the subsystem of DMS and non-DMS wells become almost totally uncoupled one from the other.

II. EXPERIMENT

The structures used in this investigation were grown by MBE on a 2-μm ZnSe buffer layer, deposited directly on GaAs (100) substrates. Symmetric MQW structures were fabricated using ZnSe layers for the barriers and nonmagnetic $Zn_{1-x}Cd_xSe$ and magnetic $Zn_{1-x-y}Cd_xMn_ySe$ layers for the wells. For triple QW's two complementary structures were fabricated, with the $Zn_{1-x-y}Cd_xMn_ySe$ layers used either for the center well (sample TQW1) or for the two side wells (TQW2). Similarly, two quintuple QW's were grown, with DMS layers used either for the central well (QQW1) or for the second and fourth wells (QQW2). Similar dimensions were used for the barriers and for the wells. After depositing the MQW's, the structures were capped by a 1-μm ZnSe protective layer. Parameters for these multiple QW's are given in Table I, and the structures are schematically shown in Fig. 1, where the DMS and non-DMS wells are indicated as darkly and lightly shaded regions, respectively.

Since the band-edge splitting shown by $Zn_{1-x-y}Cd_xMn_ySe$ layers in a magnetic field will play a central role in this study, it is important to discuss at the outset the Zeeman splittings occurring in the DMS layer in some detail. It was shown that the effective spin of the manganese ions, which determines the Zeeman splitting in DMS's, is practically independent of the host crystal[30] (i.e., it is essentially the same in $Zn_{1-y}Mn_ySe$, $Zn_{1-y}Mn_yTe$, or $Cd_{1-y}Mn_ySe$ for the same y). The Zeeman splitting in $Zn_{1-x-y}Cd_xMn_ySe$ layers with $y \approx 0.04$ used in this work will thus be very similar to that in $Zn_{1-y}Mn_ySe$ with $y \approx 0.04$. The Zeeman splitting of the band edge of $Zn_{1-y}Mn_ySe$, $y \approx 0.04$ for the conduction and the heavy-hole band determined experimentally in earlier studies[14] is shown as a function of magnetic field in Fig. 2. This variation indicates how the depth of DMS wells in the MQW structures will change with field for the two spin orientations. The much larger Zeeman shift of the heavy-hole band, characteristic of II-VI-based DMS's, is clearly evident.

To perform optical transmission experiments on the MQW samples, the GaAs substrate had to be removed. This was done by mechanical polishing, followed by selective chemical etching in 1:20 $NH_4OH:H_2O_2$ solution at room temperature. The interband magnetoabsorption experiments were performed in an optical cryostat ($T \geqslant 1.5$ K) equipped with a 6-T superconducting magnet. The light source used in the experiments was a halogen lamp together with a 1-m monochromator. The monochromatic light was circularly polarized, so as to allow the identification of transitions between different spin states. The signal was detected by a photomultiplier tube and was sent to a lock-in amplifier and a computer-controlled analyzer for data storing and processing.

III. WAVE-FUNCTION DISTRIBUTIONS IN SYSTEMS OF UNEQUAL WELLS

For a detailed description of the observed transitions in MQW's, we need to know the correct potential profile of the systems at all fields. Since $Zn_{1-x-y}Cd_xMn_ySe$ well layers contain 4% of Mn^{2+}, the well depth of these layers is in fact slightly different from the nonmagnetic $Zn_{1-x}Cd_xSe$ wells even at zero magnetic field, due to the (slightly) different band gap of $Zn_{1-x-y}Cd_xMn_ySe$ and the (slightly) different strain condition in that layer. Because these differences are small on the scale of the well depth, our triple and quintuple QW's are very nearly resonant at zero and/or low field. The eigenenergies and the corresponding wave functions of these

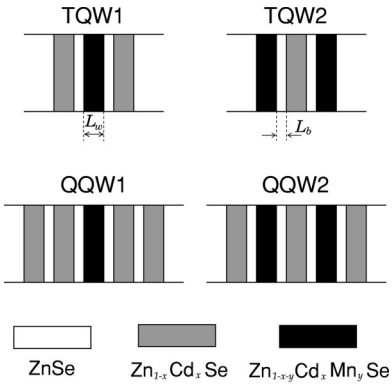

FIG. 1. Schematic diagrams for the symmetric multiple QW's (TQW1, TQW2, QQW1, and QQW2) consisting of $Zn_{1-x-y}Cd_xMn_ySe$ and $Zn_{1-x}Cd_xSe$ wells, with ZnSe barriers. Shaded regions indicate wells (dark color for $Zn_{1-x-y}Cd_xMn_ySe$, light color for $Zn_{1-x}Cd_xSe$ wells), and unshaded regions are ZnSe barriers.

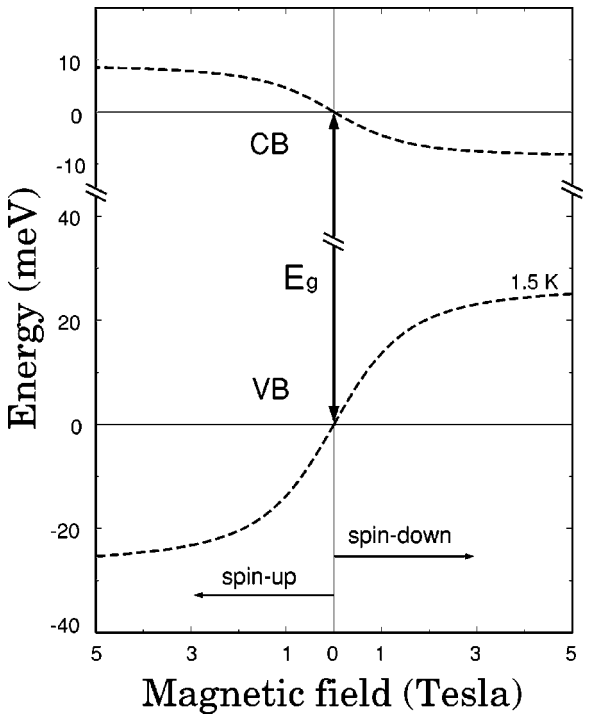

FIG. 2. Calculated band-edge splitting of the conduction and the heavy-hole bands in $Zn_{1-y}Mn_ySe$ with $y \approx 0.04$. The regions to the left and to the right of $B=0$ show the behavior of the spin-up and the spin-down band edges, respectively. E_g is the energy gap at $B=0$.

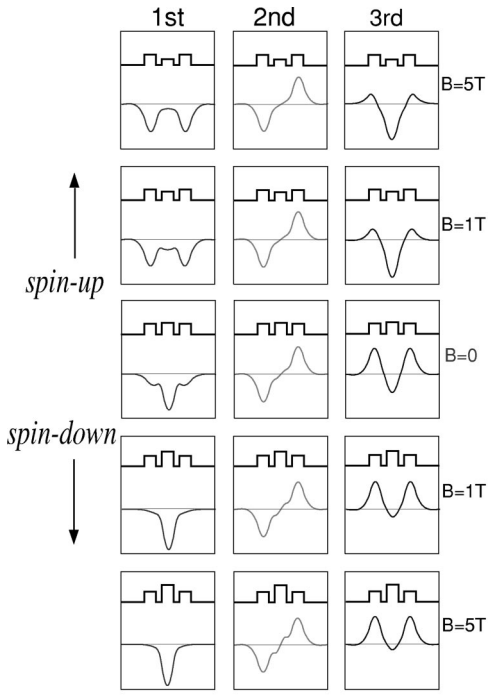

FIG. 3. Progression of potential profile with magnetic field, and corresponding wave functions for the heavy-hole band, for spin-up and spin-down states in TQW1. The first, second, and third columns correspond to the first, second, and third states of the ground-state triplet, respectively. Noticeable qualitative changes in heavy-hole localization occur in the first and the third states.

structures at zero field are thus very similar to the case of three or five *identical* QW's. This property allowed us to treat these systems in Ref. 19 as consisting of essentially identical wells when the Zeeman splitting was small. However, Zeeman splittings of the band edges in the DMS layers at low temperatures can be so large that they may no longer be treated as perturbations of the ''original'' (i.e., zero-field) well depths. At low temperatures even moderate fields (e.g., 1 T) transform a given MQW system comprised of DMS and non-DMS wells into a combination of unequal wells, especially in the heavy-hole band. This results in a situation where not all wells are in resonance with one another, which greatly affects both the nature of the coupling between the wells and the distribution of electron probability throughout the system.

When a magnetic field is applied, it is evident from Fig. 2 that most of the potential variation in the DMS wells occurs in the heavy-hole band, while the conduction-band wells experience considerably less change. At the same time, the conduction-band wells in our structures are much deeper than wells in the valence band (approximately 200 meV, as compared to 50 meV at $B=0$). Consequently, magnetic field has relatively little effect on conduction-electron states and on their wave-function distribution. In contrast, in the heavy-hole band major changes take place in the DMS well potential when the field is applied, due to the *combined* effects of a relatively small band offset and a much larger Zeeman splitting characteristic for that band. This results in very significant, *qualitative* changes in the heavy-hole wave functions of the MQW's.

We will use the case of TQW1 to illustrate this behavior. The calculated band-edge profiles for the heavy-hole band at $B=0$ (including the effect of strain) are shown for TQW1 in the third row of panels in Fig. 3. The corresponding wave functions for the three lowest heavy-hole states are also shown in that row. At $B=0$ the lowest state (h_1) is clearly distributed over the three wells, while the second state (h_2) is localized only in the two side wells. The third state (h_3) is again distributed over the three wells.

The evolution of the potential profile for spin-up and spin-down heavy-hole states with increasing field is shown for TQW1 in the upper (first and second) and the lower (fourth and fifth) rows of Fig. 3, respectively. We first consider the spin-down states at high fields, where the central well becomes significantly deeper than the side wells, resulting in a symmetric triple QW system with very unequal well depths. In this configuration the central well and the side wells are no longer resonant with each other, and the coupling between them is dramatically reduced. We now have, effectively, a combination of a single (central) QW and a double-resonant QW comprised of the side wells. The wave function of the h_1 state then approaches the ground-state wave function of a single quantum well, localized only in the central DMS layer due to the significantly lower potential of that layer compared to the side wells. The h_2 and h_3 wave functions, on the other hand, are mostly localized in the two side wells, and are thus determined primarily by those wells. This is not surprising for the h_2 state, since that state originates from one localized in the two side wells of the triple QW with equal well depths.[19] However, the wave function of h_3, which was initially nearly equally distributed over the three wells, has now also redistributed itself primarily into the two

side wells. This process of wave-function redistribution and its evolution can be readily probed in our experiment.

In contrast, the depth of the DMS well in TQW1 for the spin-up state is significantly shallower at high magnetic field than that of the side wells, and the whole system now begins to separate into a deep double-resonant quantum well originating from the side wells (for which the central well, no longer in resonance, becomes part of the barrier) and a single shallow central QW. Then the lowest state h_1 and the second state h_2 become those of a double QW, localized equally in the two side wells (which in the case of TQW1 correspond to the non-DMS wells), as shown in the first and second columns of the top panels in Fig. 3. Surprisingly, most of the wave function for the h_3 state is seen to localize in the central well, even though that well is at the highest potential.

The complete qualitative redistribution of wave functions of the h_1 and h_3 states in TQW1 in the large perturbation region can be produced continuously by varying an external magnetic field. Similar wave-function redistributions are obtained for the other QW geometries used in this investigation. Thus in the case of TQW2 (see Fig. 1), potential variations occur in the two side wells as the magnetic field is applied. For spin-down states, the two side wells in the heavy-hole band in this sample become much deeper than the center well. In this case the h_1 wave function transfers almost entirely into the two side wells, eventually becoming the same as the h_2 wave function, only with opposite parity—mirroring qualitatively the *spin-up* behavior of TQW1. For spin-up states of TQW2, the two side wells become much shallower than the center well, and the wave function of h_1 becomes mostly localized in the center well as the field increases, resembling (not surprisingly) the spin-down behavior of TQW1 discussed above.

Using similar arguments and referring to Fig. 1, it is readily seen that when the applied magnetic field is in the strong perturbation limit the QQW1 structure will split into a single QW and two identical pairs of resonant double QW's; and QQW2 will separate into a resonant triple QW made up of non-DMS material and a resonant DMS double QW. This splitting into subgroups will be manifested by characteristic optical behavior discussed below.

IV. OPTICAL TRANSITIONS IN MULTIPLE QW SUBGROUPS

A. Triple quantum wells

Figure 4 shows transition energies for the TQW1 sample as a function of applied magnetic field for the two circular polarizations. The solid lines show transition energies calculated for TQW1, obtained by taking the Zeeman splitting shown in Fig. 2 as the potential variation of the DMS wells. The calculations in Fig. 4 are done using the $\mathbf{k}\cdot\mathbf{p}$ model and the ''finite element method.''[31] The versatility of the latter algorithm, and its suitability for investigating systems of this type, was discussed in Ref. 27. Since the structures considered here have more layers (i.e., more elements) than double QW's, a great amount of computing time would be required if all eight bands were to be taken into account, as was done for the double wells. Since our interest is to understand *trends*, which such system display as the well depths begin to differ, and since we are dealing with a wide-gap semiconductor system where interactions with remote bands are weak, in the calculations we have used a single-band model. This approach has the added advantage of keeping the physics of the system clearly in evidence. In order to allow comparison with experimental data, we have also included the effect of strain and of the small but finite difference between the band edges of the DMS and non-DMS wells at zero magnetic field. The parameters used have been discussed in Ref. 19, and the reader is referred to that reference for details.

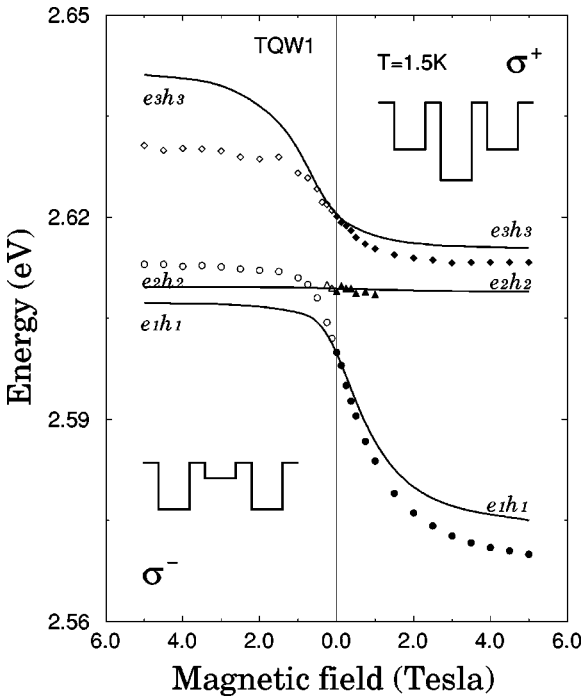

FIG. 4. Calculated energies of the $\Delta n=0$ transitions for TQW1, plotted together with experimental results. The solid lines are calculated for actual structures used in the experiments, taking into account their detailed phyical properties (strain, exact band alignment at $B=0$), as discussed in the text.

Calculated energies for optical transitions involving the ground-state triplet in the TQW1 configuration (i.e., DMS layer in the center well) exhibit several interesting phenomena, that were not present in the small perturbation regime discussed in Ref. 19. One of the most striking features is the asymmetry of the Zeeman shift between the σ^+ and σ^- polarizations (i.e., the spin-down and spin-up transitions, respectively) exhibited by both e_1h_1 and e_3h_3 transitions. For the σ^+ polarization, the e_1h_1 transitions in the TQW1 configuration show the largest Zeeman shift, indicating that states involved in these transitions are much more localized in the DMS wells than other states. For the σ^- polarization, however, the e_1h_1 transition shows considerably smaller Zeeman splittings and quickly saturates at magnetic fields higher than 0.75 T, indicating that now the states involved in this transition reside primarily in the non-DMS layers. A similar asymmetry of the Zeeman shift, but in the opposite direction, is also observed for the e_3h_3 transition.

This asymmetric behavior of the e_1h_1 and e_3h_3 transitions, which differ from their behavior in the small perturbation regime (where the Zeeman shift is approximately symmetric), results from the difference in the distribution of the

wave functions for the spin-up and spin-down states (see Fig. 3). This feature is characteristic of coupled MQW systems made up of DMS and non-DMS combinations, including superlattices.[12,13] In a single QW consisting of DMS material, the ground state is always localized in the well, even though the well depth changes with magnetic field for different spin states. In multiwell systems, however, the lowest-lying state seeks out wells of the lowest potential, to which it tunnels when the well depths change relative to one another. Such wave-function transfer taking place in a triple QW structure is clearly seen for the h_1 and h_3 states in the first and the third columns of Fig. 3.

A fundamental feature of the TQW1 configuration can be appreciated by examining the three transition energies at 5 T for both σ^+ and σ^- polarizations. It is clear in that limit that two of the transitions are always close to each other, while a third one is farther removed. The former resemble the two lowest-energy transitions of a double QW, while the latter behaves like the ground-state transition of a single QW. This *subgroup* behavior results from the significant reduction in the coupling between the central and the side wells. In triple QW's under resonant conditions, all wells are strongly coupled to one another, and the states of the lowest multiplet are almost equally separated, as is the case for zero magnetic field in Fig. 4. However, as the well moves away from subgroups resonance, their behavior becomes (nearly) independent from each other. Then each subgroup of QW's exhibits their own characteristics, without ''feeling'' the existence of the other QW's. In the case of the TQW1 configuration the system divides itself, due to the large potential variation of the DMS band edges with magnetic field, into a single QW made of the DMS layer and a double quantum well consisting of non-DMS materials.

Since the ''single QW subgroup'' corresponds to the DMS well, the state representing the single quantum well behavior will always follow the magnetic shift of the DMS material. This behavior is clearly demonstrated in Fig. 4, where the e_1h_1 transition for σ^+ and the e_3h_3 transition for σ^- clearly follow the Zeeman shift characteristic of the DMS layer and show a different behavior than the other two transition lines. The transitions corresponding to the ''double QW subgroup'' shows a different characteristic behavior. The flatness of the energy versus field behavior of the two closely-spaced transitions reflects the fact that states participating in these transactions reside in the non-DMS $Zn_{1-x}Cd_xSe$ side wells. The difference in the transition doublets for the two spin orientations (e_1h_1 and e_2h_2 for σ^-; e_2h_2 and e_3h_3 for σ^+) arises from the fact that—even though the wells are identical—the behavior for the interwell coupling in this double QW subgroup is different for the two spin orientations is magnetic-field dependent. In particular, it is clear from the larger separation exhibited by the transition energies in the σ^+ polarization that the coupling through a barrier containing a deep well is stronger than that through the more ''solid'' barrier, as is the case for σ^-.

Experimental data observed for TQW1 in magnetotransmission are shown by points in Fig. 4. The observed magnetic-field dependences of the transitions agree qualitatively with the calculations. First, the calculated asymmetry of the Zeeman splitting between transitions for the σ^+ and σ^- polarizations is indeed observed for the e_1h_1 transition.

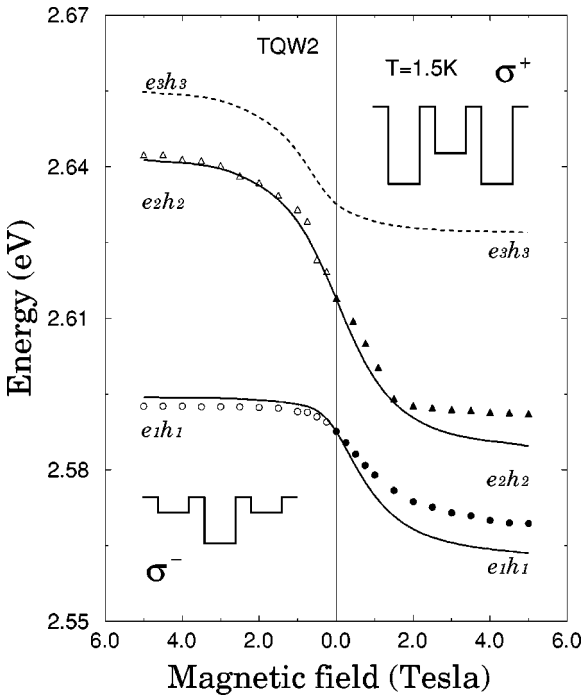

FIG. 5. Calculated energies of the $\Delta n = 0$ transitions for TQW2, plotted together with experimental results. The solid lines are calculated for actual structures used in the experiments, taking into account their detailed physical properties (strain, exact band alignment at $B = 0$), as discussed in the text.

Furthermore, by careful inspection of experimental data, one can also see (especially for the low-field region in the σ^+ polarization) that the transitions for this triple QW divide into subgroups in a continuous manner as the magnetism is increased, essentially corroborating the wave-function picture of this system under large perturbation.

Another noticeable feature observed in the TQW1 spectra is the disappearance of the e_2h_2 transition as it approaches the e_1h_1 transition for the σ^- polarization and as it comes close to the e_3h_3 transition for the σ^+ polarization. This may be due to the near merging of the h_2 state with h_1 for the spin-up configuration and with h_3 for the spin-down configuration, respectively.

In the TQW2 configuration, the situation at zero magnetic field is identical to the TQW1 case but becomes quite different when a magnetic field is applied, since now the two side wells will undergo a change in the well depth. Calculated results are shown for TQW2 as solid and dotted lines in Fig. 5 for the observed and the not observed transitions, respectively. The system also divides into two subgroups (a single quantum well and a double quantum well) when a high magnetic field is applied. The band alignment of the system at 5 T is schematically shown by insets in the figure for σ^+ and σ^- polarizations. In this configuration, however, the double QW is now made of DMS layers, and the single quantum well is non-DMS. Thus the two eigenstates related to the double quantum well will show large Zeeman shifts, while the eigenstate involving the single central QW will undergo negligible Zeeman splittings. Such behavior is clearly seen in Fig. 5, where two lines (e_1h_1 and e_2h_2 for the σ^+ polarization and e_2h_2 and e_3h_3 for the σ^- polarization) move together, and one line (e_3h_3 for the σ^+ polarization and e_1h_1

for the σ^- polarization) is significantly separated from this doublet, showing only a weak-field dependence.

The experimental absorption spectrum observed for TQW2 shows only two transitions at zero magnetic field (except for the light-hole transition at higher energy, which we do not discuss), as shown in the figure. The two observed peaks are attributed to the e_1h_1 and e_2h_2 transitions, i.e., to the most probable transitions according to the $\Delta n=0$ selection rule. Here one also observes the asymmetry of the Zeeman splitting of the e_1h_1 transition for the two polarizations, similar to that seen in TQW1. The distinctive feature of TQW2 is that the *largest* Zeeman splitting is observed for the e_2h_2 transition, rather than for the ground-state transition e_1h_1. This indicates that the e_2 and h_2 states are more localized in the two DMS side wells than the other states, as is, of course, expected from Fig. 3. Furthermore, the Zeeman splitting of the e_2h_2 transition in TQW2 is nearly *symmetric*. The reason for that is, as we saw, the wave functions of the e_2 and h_2 states are not allowed to leak to the central well—even when the central well potential is significantly lower than the side well. These wave functions thus always remain in the two side wells for both spin-up and spin-down states (as shown for the h_2 state in the second column of Fig. 3), essentially reflecting the behavior of the band edges of the DMS material for the two spin orientations. This results in the observed symmetric Zeeman splitting of the e_2h_2 transition.

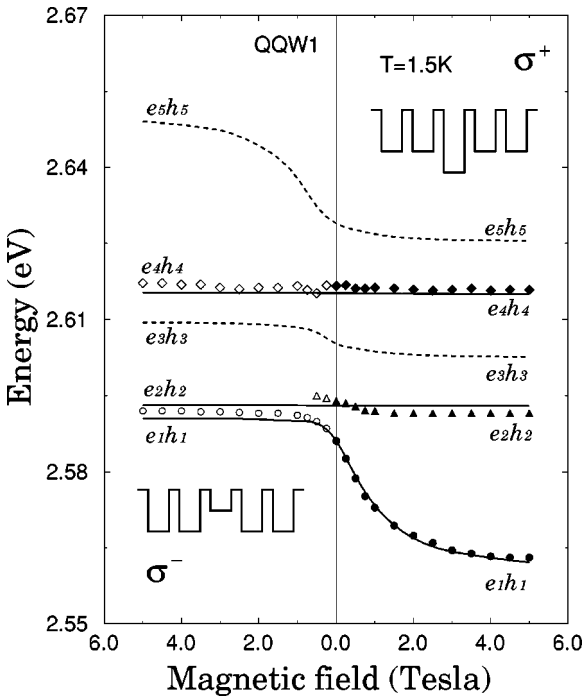

FIG. 6. Calculated energies of the $\Delta n=0$ transitions for QQW1, plotted together with experimental results. The solid lines are calculated for actual structures used in the experiments, taking into account their detailed physical properties (strain, exact band alignment at $B=0$), as discussed in the text.

B. Quintuple quantum wells

In the quintuple QW's, the QQW1 structure is very similar to TQW1, because in both structures the central well consists of a DMS layer. The calculated behavior of e_nh_n transitions for QQW1 in a magnetic field is shown in Fig. 6, where the e_1h_1 transition (experiencing an asymmetric Zeeman splitting) and e_2h_2 transition (no Zeeman splitting) exhibit almost identical behavior to that already seen in TQW1. This similarity of transitions involving the lowest two states ($n=1,2$) in TQW1 and in QQW1 can be expected by comparing wave functions of these states in triple and quintuple QW's. Consistent with the tendency to separate into independent subgroups at high magnetic field, the wells of the QQW1 system also divide into a single QW and a *pair of double* QW's, both subgroups acting nearly independently from each other. The band profiles of QQW1 at 5 T for both spin-up and spin-down states are shown schematically in the Fig. 6 as insets.

It is instructive to consider the calculated splittings shown in Fig. 6 in some detail. First, there is a splitting due to the interaction *within* each pair of double QW's. This is responsible for the doublets (e_2h_2, e_3h_3) and (e_4h_4, e_5h_5) on the right, and for the doublets (e_1h_1, e_2h_2) and (e_3h_3, e_4h_4) on the left of the figure. These pairs of lines (which have a close resemblance to the lines originating from the double QW subgroup in Fig. 4) are further split by the resonant interaction between the two pairs of QW's in Fig. 6.

One should notice that the energy splitting within the two doublets is different for the two spin states at high magnetic field. For example, the splitting between the e_1h_1 and e_2h_2 transitions for spin-up states, on the left side of Fig. 6, is much smaller than for the other doublets. One can understand this as follows. For the σ^+ polarization, the two side double QW's are coupled through a barrier containing a *deep* center well, so that both lowest states can interact across the center well. Thus the coupling strength for both states will be similar and will result in almost the same energy splitting, as is indeed seen in the figure (compare the separation between e_2h_2 and e_3h_3 and that between e_4h_4 and e_5h_5). For the σ^- polarization, however, the energy separation between two of the transitions (e_1h_1 and e_2h_2), involving the lowest two energies, is much smaller than that between e_3h_3 and e_4h_4, whose energy separation actually approaches that shown by the double QW interaction for the σ^+ polarization. This is because the coupling between the lowest state of the double QW is significantly weaker than that between its higher state. This difference in the degree of coupling results from the fact that for σ^- the lowest states are separated by a ''solid'' barrier, while the upper states are separated by a ''hollow'' barrier, which increases the coupling. Such increased coupling *through a barrier containing a well* (as distinguished from a ''solid'' barrier) is actually evident in all of the systems examined and provides a valuable physical insight into the interwell coupling process generally.

The QW subsystems become much more interesting in the QQW2 configuration, in which two of the wells consist of DMS layers. As one would expect, QQW2 separates into a double and a triple QW at high magnetic field, while retaining the resonant condition within each subgroup. The behavior of the transitions, and the results calculated for the separated subgroups at 5 T, are shown in Fig. 7. It can be clearly seen that the splitting between transitions of coupled states in the double QW group is different for the two spin orientations at high magnetic fields: the e_1h_1 and e_2h_2 transitions

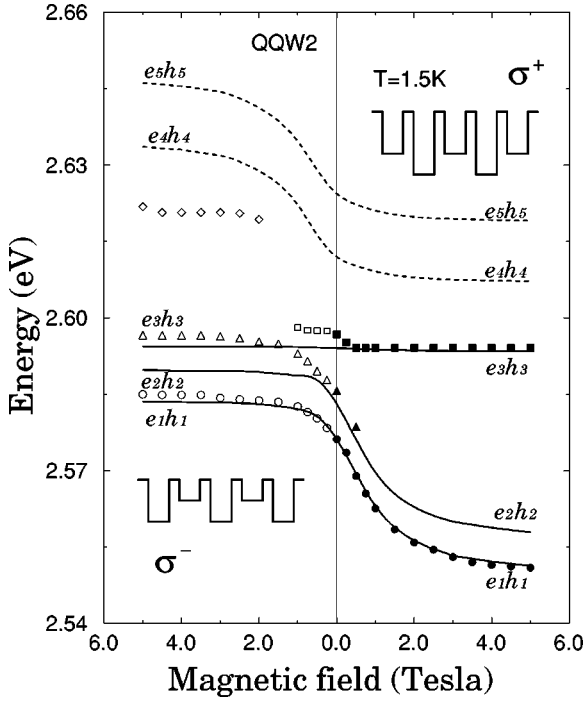

FIG. 7. Calculated energies of the $\Delta n=0$ transitions for QQW2, plotted together with experimental results. The solid lines are calculated for actual structures used in the experiments, taking into account their detailed physical properties (strain, exact band alignment at $B=0$), as discussed in the text.

for the σ^+ polarization, and the e_4h_4 and e_5h_5 transitions for the σ^- polarization correspond to an effective double QW made up of the DMS layers. However, the energy splitting between the e_1h_1 and e_2h_2 transitions in the σ^+ polarization is clearly smaller than that between e_4h_4 and e_5h_5 transitions for σ^-. Since the well and the barrier thicknesses remain the same, the difference in the energy splitting originates from the well depth. The double QW created by spin-up states (σ^-) is much shallower and is separated by a ''hollow'' barrier containing a deep well. As already noted, this results in a stronger interwell coupling within the double QW and thus in a larger splitting between the spin-up $n=4$ and $n=5$ states. The spin-down (σ^-) double QW, on the other hand, feels a more ''solid'' barrier, thus resulting in a weaker coupling between the $n=1$ and $n=2$ states. Similar considerations also account for the differences in the energy separations for the σ^+ and σ^- transitions in the triple well subsystem of QQW2, seen in Fig. 7.

Notice that the Zeeman shift of the lowest ($n=1$) transition for the σ^+ polarization in Fig. 7 is almost the same as that calculated for the highest ($n=5$) transition for σ^- and that the very weak dependence on magnetic field of the highest ($n=5$) state transition for the σ^+ polarization is similar to that of the lowest ($n=1$) state transition for the σ^- polarization. This behavior of the lowest and the highest states is actually common for all multiple QW's investigated in this study, as clearly seen in Figs. 4–7.

In the experiments, we were not able to observe all the transitions involving the lowest quintuplet of states in the quintuple QW's. Specifically, in neither of these samples did we observe transitions involving the highest (e_5 and h_5) states. This may be due to the weak intensity and/or to the possible overlap of these transitions with the light-hole transition. However, it is in fact remarkable that we can separately resolve most of the individual transitions originating from a multiplet of states that already approaches a *superlattice* subband. In both quintuple QW's the asymmetry in the Zeeman shift of the e_1h_1 transition is clearly observed, very similar to that shown by the triple QW's. In addition, almost complete lack of dependence on magnetic field is seen for two transitions in QQW1 (e_2h_2 and e_4h_4), and of the e_3h_3 transition in QQW2. Unfortunately, the lack of resolution of transitions involving the higher levels of the ground-state quintuplet does not warrant more detailed discussion of these very interesting structures.

V. CONCLUDING REMARKS

We investigated symmetric multiple (triple and quintuple) arrays of QW's as a function of large variation of well depth by means of using DMS layers for some of the wells. By applying strong magnetic fields at low temperatures (1.5 K), we were able to investigate the transformation of the MQW system into subsets of resonant quantum wells, with *redistribution* of the wave function within each subset separately. For example, in triple QW's the system separates into a single QW and a double QW with clearly identifiable, nearly independent behaviors; and in the case of quintuple QW's we similarly observed separation into either a single QW and a pair of double QW's (QQW1), or a double QW and a triple QW (QQW2). The results persistently show that, if two or more wells are in resonance but are separated by a barrier that itself contains another well, the coupling is stronger than if there was no well in the barrier; and the strength of the coupling increases with the depth of the intervening (nonresonant) well.

We note parenthetically that in studying MQW's we are automatically dealing with a configuration that begins the process of forming a superlattice. When the wells are equal (or nearly so), the multiplet of states discussed in this paper corresponds to a lowest superlattice subband, the lowest and the highest states of the multiplet corresponding to the $q=0$ and $q=1$ points of such a superlattice subband in k space. In the region of strong magnetic fields, on the other hand, the MQW's studied in this paper can be viewed as analogous to a superlattice consisting of *two kinds* of wells. Thus the separation of MQW properties into those associated with subgroups of resonantly coupled wells illustrates the process of a subband splitting in such superlattices into *two modes*—one related to the shallow, the other to the deep wells. As the deep wells (DMS layers in σ^+ configuration) transform to shallow (DMS layers in σ^-), clear anticrossing of the subbands is observed in the low-field region, as born out by the calculated and observed behavior in Figs. 4–7.

Finally, in comparing MQW's and superlattices, one should also point out an important difference between the two. In a superlattice every quantum well is by assumption identical, and thus the electron probability is also the same in each well. In a MQW, on the other hand, the wave functions are distributed *unequally* between the various wells, as we have emphasized throughout this paper. However, inspection of Fig. 2 in Ref. 19 will show that the wave functions are (approximately) equal in the lowest and highest state of a

given multiplet. Since in practice every superlattice is necessarily a MQW, it thus follows that the assumption of equivalent wells does indeed hold for $q = 0$ (lowest state of the multiplet) and $q=1$ (highest state) for each subband; but that it fails for $0 < q < 1$. The consequences of this are unclear (most optical properties of superlattices are determined by subband *extrema*), but studies of intermediate excited states in MQW's (such as e_2, h_2 for triple QW's or e_i, h_i with $i = 2, 3, 4$ in quintuple QW's studied in this paper) provide an opportunity to investigate the behavior of superlattice states at intermediate values of q within the SL Brillouin zone.

ACKNOWLEDGMENTS

The authors are grateful to H. Luo and G. Yang for many fruitful discussions. This work was supported by NSF Grant No. DMR 97-05064.

*Electronic address: Sanghoon.Lee.39@nd.edu

[1] J. K. Furdyna, J. Appl. Phys. **64**, R29 (1988).
[2] J. A. Gaj, in *Diluted Magnetic Semiconductors*, edited by J. K. Furdyna and J. Kossut, Semiconductors and Semimetals Vol. 25 (Academic, Boston, 1988), Chap. 7.
[3] A. Petrou, W. C. Chou, X. C. Liu, J. Warnock, and B. T. Jonker, J. Lumin. **52**, 175 (1992).
[4] S. Datta, J. K. Furdyna, and R. L. Gunshor, Superlattices Microstruct. **1**, 327 (1985).
[5] L. P. Fu, S. T. Lee, A. Petrou, J. Warnock, and B. T. Jonker, Phys. Rev. B **50**, 4696 (1994).
[6] J. A. Gaj, W. Grieshaber, C. Bodin-Deshayes, J. Cibert, Y. Merle d'Aubigné, and A. Wasiela, Phys. Rev. B **50**, 5512 (1994).
[7] V. V. Rossin, T. Böttger, and F. Henneberer, Phys. Rev. B **54**, 7682 (1996).
[8] P. J. Klar, D. Wolverson, J. J. Davies, W. Heimbrodt, and M. Happ, Phys. Rev. B **57**, 7103 (1998).
[9] H. H. Cheng, R. J. Nicholas, M. J. Lawless, D. E. Ashenford, and B. Lunn, Solid-State Electron. **40**, 69 (1996).
[10] D. R. Yakovelev, Solid-State Electron. **40**, 34 (1996).
[11] X. Liu, A. Petrou, J. Warnock, B. T. Jonker, G. A. Prinz, and J. J. Krebs, Phys. Rev. Lett. **63**, 2280 (1989).
[12] B. T. Jonker, X. Liu, W. C. Chou, A. Petrou, J. Warnock, J. J. Krebs, and G. A. Prinz, J. Appl. Phys. **69**, 6097 (1991).
[13] N. Dai, H. Luo, F. C. Zhang, N. Samarth, M. Dobrowolska, and J. K. Furdyna, Phys. Rev. Lett. **67**, 3824 (1991).
[14] N. Dai, L. R. Ram-Mohan, H. Luo, G. L. Yang, F. C. Zhang, M. Dobrowolska, and J. K. Furdyna, Phys. Rev. B **50**, 18 153 (1994).
[15] J. F. Smyth, D. A. Tulchinsky, D. D. Awschalom, N. Samarth, H. Luo, and J. K. Furdyna, Phys. Rev. Lett. **71**, 601 (1993).
[16] C. Juang, R. Y. Hwang, H. C. Pan, C. M. Chang, and B. J. Lee, J. Appl. Phys. **70**, 4973 (1991).
[17] S. Fukuta, H. Goto, N. Sawaki, T. Suzuki, H. Ito, and K. Hara, Semicond. Sci. Technol. **8**, 1881 (1993).
[18] T. Kai, M. Morifuji, M. Yamaguchi, and C. Hamaguchi, Semicond. Sci. Technol. **9**, 1465 (1994).
[19] S. Lee, M. Dobrowolska, J. K. Furdyna, and L. R. Ram-Mohan, Phys. Rev. B **59**, 10 302 (1999).
[20] R. Dingle, A. C. Gossard, and W. Wiegmann, Phys. Rev. Lett. **34**, 1327 (1975).
[21] N. Debbar, S. Hong, J. Singh, and P. Bhattacharya, and R. Sahai, J. Appl. Physiol. **65**, 383 (1988).
[22] A. Yariv, C. Lindsey, and Uri Sivan, J. Appl. Physiol. **58**, 3669 (1985).
[23] H. Kawai, K. Kaneko, and N. Watanabe, J. Appl. Phys. **58**, 1263 (1975).
[24] T. Kamizato and M. Matsuura, Phys. Rev. B **40**, 8378 (1989).
[25] P. Bonnel, P. Lefebvre, B. Gil, H. Mathieu, C. Deparis, J. Massies, G. Neu, and Y. Chen, Phys. Rev. B **42**, 3435 (1990).
[26] J. F. Smyth, D. D. Awschalom, N. Samarth, H. Luo, and J. K. Furdyna, Phys. Rev. B **46**, 4340 (1992).
[27] S. Lee, M. Dobrowolska, J. K. Furdyna, H. Luo, and L. R. Ram-Mohan, Phys. Rev. B **54**, 16 939 (1996).
[28] I. Lawrence, G. Feuillet, H. Tuffigo, C. Bodin, J. Cibert, P. Peyla, and A. Wasiela, Superlattices Microstruct. **12**, 119 (1992); Mater. Sci. Eng., B **16**, 235 (1993).
[29] W. Heimbrodt, O. Goede, Th. Köpp, K. Hieke, H.-E. Gumlich, Th. Pier, B. Lunn, and T. Gregory, J. Cryst. Growth **117**, 859 (1992).
[30] J. A. Gaj, C. Bodin-Deshayes, P. Peyla, J. Cibert. G. Feuillet, Y. Merle d'Aubigne, R. Romestain, and A. Wasiela, *Proceedings of the 21st International Conference on the Physics of Semiconductors* (World Scientific, Singapore, 1992), p. 1936.
[31] L. R. Ram-Mohan, S. Saigal, D. Dossa, and J. Shertzer, Comput. Phys. **4**, 50 (1990).